

Balancing Robustness and Responsiveness in a Real-time Indoor Location System using Bluetooth Low Energy Technology and Deep Learning to Facilitate Clinical Applications

Guanglin Tang, Yulong Yan, Chenyang Shen, Xun Jia, Meyer Zinn, Zipalkumar Trivedi, Alicia Yingling, Kenneth Westover, Steve Jiang

Medical Artificial Intelligence and Automation (MAIA) Laboratory, Department of Radiation Oncology, University of Texas Southwestern Medical Center, Dallas, TX 75235, United States of America

* Corresponding Author: Guanglin.Tang@utsouthwestern.edu

Abstract

An indoor, real-time location system (RTLS) can benefit both hospitals and patients by improving clinical efficiency through data-driven optimization of procedures. Bluetooth-based RTLS systems are cost-effective but lack accuracy and robustness because Bluetooth signal strength is subject to fluctuation. We developed a machine learning-based solution using a Long Short-Term Memory (LSTM) network followed by a Multilayer Perceptron classifier and a posterior constraint algorithm to improve RTLS performance. Training and validation datasets showed that most machine learning models perform well in classifying individual location zones, although LSTM was most reliable. However, when faced with data indicating cross-zone trajectories, all models showed erratic zone switching. Thus, we implemented a history-based posterior constraint algorithm to reduce the variability in exchange for a slight decrease in responsiveness. This network increases robustness at the expense of latency. When latency is less of a concern, we computed the latency-corrected accuracy which is 100% for our testing data, significantly improved from LSTM without constraint which is 96.2%. The balance between robustness and responsiveness can be considered and adjusted on a case-by-case basis, according to the specific needs of downstream clinical applications. This system was deployed and validated in an academic medical center. Industry best practices enabled system scaling without substantial compromises to performance or cost.

1. Introduction

Indoor Real-time Location Systems (RTLS) that enable precise position tracking are beneficial in many fields. In industrial manufacturing, an RTLS enables autonomous robots to navigate towards designated locations or other objects whose locations the RTLS tracks simultaneously [1]. In malls and public transit, it allows managers to track assets in the field and

analyze and predict customer traffic to provide adequate time to prepare for their arrival [2]. In clinical environments, an RTLS can increase workflow efficiency and improve patient safety by, for example, facilitating rapid searching of equipment and accessories, which reduces the time spent locating items for procedures. An RTLS also helps deliver health care more efficiently, reduces clinical errors, and enhances patient safety by monitoring patients' locations, enabling a rapid response by healthcare providers in the event of a medical emergency [3] [4] [5]. In the Radiation Oncology building (ERO) at the University of Texas Southwestern Medical Center (UTSW), we already use an in-house RTLS to automatically check the location of patients and accessories before scheduled delivery of radiotherapy to ensure it proceeds as planned. Additionally, historical location records of staff, patients, and equipment can help detect and reduce the effects of radiation exposure and disease infection by determining who may have been exposed within a given time frame.

Real-time location tracking can be achieved through several methods, including choke-point schemes [6] [7] [8], time-difference-based schemes [9] [10] [11], and signal strength-based schemes [12] [13] [14]. We present a variation of the signal strength-based scheme, using Bluetooth Low Energy (BLE) as an observable signal [15] [16] [17] [18]. Our approach uses relatively mature technology that is widely available commercially, which reduced the cost of adoption. BLE has been widely used in wireless data transmission for years with iterative improvements in protocol and hardware implementation. The battery life of a low-cost (~\$10) BLE beacon can easily span years. The BLE sensors are also inexpensive (~\$10 each) and industrially mature with easy connections to computers using common protocols such as USB and simple software control using protocols written with C, Java, Python, Go, etc. Thus, it is relatively uncomplicated to deploy a reliable RTLS with many BLE devices to increase signal collection, and thus location accuracy, while minimizing upfront costs and effort spent on software development.

Most existing BLE-based RTLS solutions suffer from low accuracy (a few meters), presumably because of the noisy nature of BLE signals due to strong interference [19], which makes the system insufficient for clinical use. We developed an RTLS that utilizes the high density of sensors available and employed deep learning techniques to improve its accuracy at the zone level, which is a more useful metric for clinical applications than absolute coordinates. By identifying the zone containing a BLE beacon, our RTLS provides useful, accurate insights for clinical applications without complex setup procedures.

We have preliminarily studied the deep learning algorithms used to compute location in the BLE-based RTLS and compared the results with traditional methods, such as thresholding methods (where location is computed as the location of the scanner that receives the maximum BLE signals) and trilateration methods [12]. Our results showed that deep learning algorithms outperform the traditional methods in terms of accuracy of zone prediction, primarily because deep learning algorithms reduce the systematic error caused by infrastructure in traditional methods by fitting the function that directly maps the signals (the so-called footprint) to the location. However,

that study focused on a small clinic area comprising a single floor and 21 zones. In addition, we evaluated accuracy for each zone separately, which only tests cases in which objects never move to other zones. In the real world, a clinic building usually contains multiple floors and hundreds of zones, and objects do move across zones. Because the algorithm was trained for each zone separately, when an object crosses zones, it is very likely that the algorithm will be ambiguous, and the results will appear to jump. In this paper, we will demonstrate this issue and use a constraining method to reduce ambiguity and jumping. We applied our scheme to an RTLS to locate moving objects in an entire 3-floor clinic building.

This paper is structured as follows: the “Methods” section introduces the system components, data collection of experiments, and methods to improve location tracking; the “Results” section shows the results of the experiments; and the “Discussion and Conclusion” section discusses the results and presents our conclusions.

2. Methods

2.1 System description

In EROC at UTSW, we deployed a fleet of 142 Raspberry Pis to host the Bluetooth sensors. Raspberry Pis are small, robust, low-cost (\$35), and simple-to-install computers that run a Linux distribution. They are powered and connected by four 24V routing switches using power-over-Ethernet with a voltage transformer for each Pi. Thus, they require no additional 110V electric outlets, which eliminates a common safety concern for hospitals. Additionally, because we use a wired connection to communicate with the Raspberry Pis, data transmission is more reliable than with Wi-Fi, and there is no increased burden for the Wi-Fi that might affect patient and staff internet usage. The Raspberry Pis are installed in the ceiling, invisible from the ground, so they do not affect the building’s appearance.

Many RTLS implementations use fixed parts in the infrastructure, such as Wi-Fi routers, as transmitters and moving parts, such as smart phones, as receivers. While this scheme is convenient for brief applications, it is limited when it comes to mass deployment. For example, the battery life of the moving parts is extremely low (e.g., 1-2 days for smart phones) because of an excessive workload that includes continuous BLE signal scanning and communication with clouds, which makes tracking equipment infeasible. Moreover, smart phones or tags with communication functions are usually more expensive than simple active BLE beacons, and their communication with clouds is not as robust or efficient as wired devices. Thus, considering battery life and data communication efficiency, we used active BLE beacons as the moving parts, which transmit BLE signals, and Raspberry Pis as the fixed parts, which receive the signals and upload them to the cloud. By doing this, we minimized the workload on the moving parts, as they simply broadcast short messages including the ID information under a certain frequency, while the Raspberry Pis continuously scan for BLE signals and upload received messages to the cloud. Thus, our beacons can be small (e.g., coin or badge size) and can last years without needing their batteries

changed. They can be attached to equipment and accessories without affecting their normal usage or worn by patients on the wrist like a watch. The monitoring end, including Raspberry Pis and cloud computers, will also last a long time with only minimal maintenance efforts (e.g., changing broken hardware). There is no routine maintenance, such as changing batteries or storage.

To manage the software across the fleet, we employed an open-source, over-the-air (OTA) software solution called Mender, which enables reliable device telemetry and remote provisioning with minimal overhead. We tracked the status of Raspberry Pis by making them report a “heartbeat” signal to the OTA server every five minutes (period adjustable). This is convenient when the fleet comprises a few hundred or thousand devices. The Raspberry Pis located in treatment vaults were shielded with thermal-neutron-absorptive material (SWX-238 Flexi Boron) to prevent electronic damage from thermal neutrons generated by high-energy photon beams. We found that thermal neutrons often caused device malfunctions, which forced us to manually reboot them by cycling power at the switch end. Raspberry Pis in treatment rooms with high-energy photon beams can only last from a few hours to a few weeks without shielding. Shielding with material Flex Boron (25% Boron) with a thickness of 0.5 inches successfully eliminated the effect of thermal neutrons.

Figure 1 illustrates the structure and workflow of the deployed RTLS. BLE beacons rapidly broadcast signals, which are observed by the sensor fleet and transferred to a centralized server. The centralized server is a Linux virtual machine that hosts an MQTT broker for efficient and secure data communication, the Mender server, a PostgreSQL database for storing BLE signal and location data, and the locator engine for calculating locations. The location results, once available, are broadcast to downstream applications, such as clinical workflow optimization and patient safety checks.

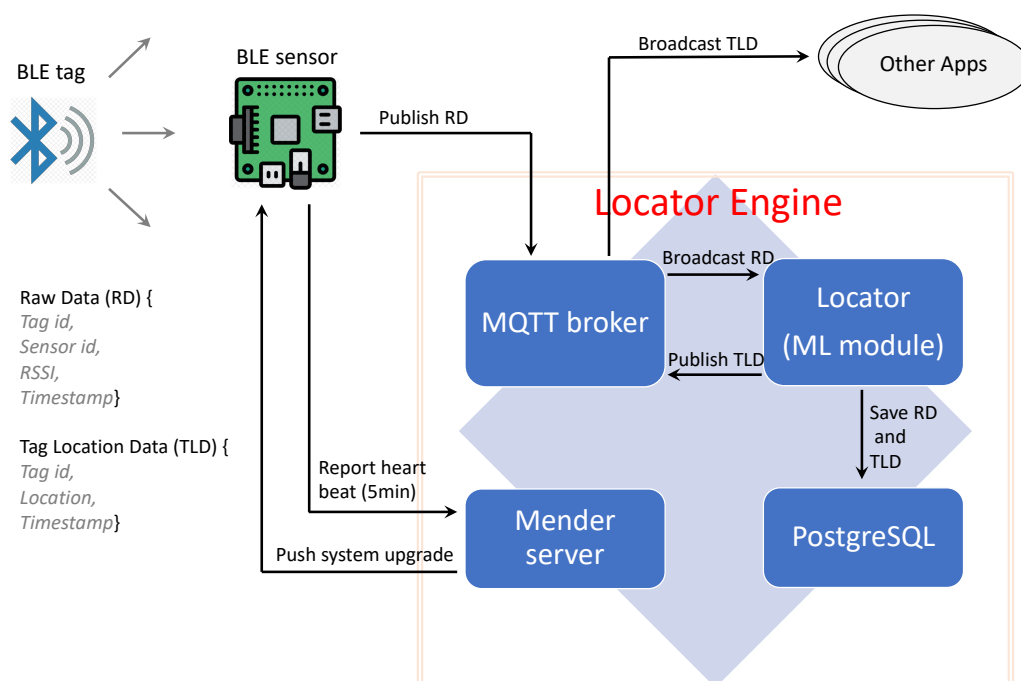


Fig. 1. Workflow of RTLS deployed in EROC at UTSW.

2.2 General methods

Although trilateration (or, following convention, triangulation) schemes work for time-difference-based RTLSs [20], their precision is much lower for signal strength-based RTLSs: they have a margin of error larger than 3 meters [21] [22] because building infrastructure and other obstructions attenuate and diffract the signal substantially relative to the traveling time. A signal strength-based RTLS uses much narrower-band signals, which increase the coherence length and, thus, the interference. For example, the coherence length of a BLE signal is over 100 m, and the wavelength of a BLE signal is about 12 cm. This means that a displacement of only a few centimeters will lead to extensive differences in signal strength. Such strong interference limits the utility of trilateration and increases the difficulty of calculating location [19]. In our experience, trilateration achieves an accuracy of approximately 50-60% in terms of zone classification on a single floor. In the multi-floor case, the accuracy is lower than 10%. We sought a deep learning technique for signal processing to improve the location accuracy by taking into account how the infrastructure influences the signal strength and by exploiting information from all sensors. This technique fits a function that directly maps the signal footprint to the location with all influences implicitly considered with hidden neurons [23].

The location calculation for our RTLS is a classification problem. At a given time, signal strengths from all 142 scanners are provided as an input, which is used to calculate the zone number (location label) as output. We first divided the building floor map into a total of 115 zones according to their functions, such as exam rooms, treatment rooms, offices, hallways, and waiting areas. These zones are meaningful in downstream applications. We then wandered around randomly in each zone while carrying BLE beacon tags and, at the same time, collected the signal strength received from all 142 scanners. The zone numbers were recorded and used to label the collected signal strength data. Figure 2 shows the floor plan of the EROC radiation oncology clinic building at UTSW with 115 zones and 142 scanners marked. We designated each exam or treatment room as a distinct zone, but we combined staff offices into larger zones because the former is more important in clinical applications than the latter. For the same reason, the scanner density is higher in the clinical areas than in the staff office areas.

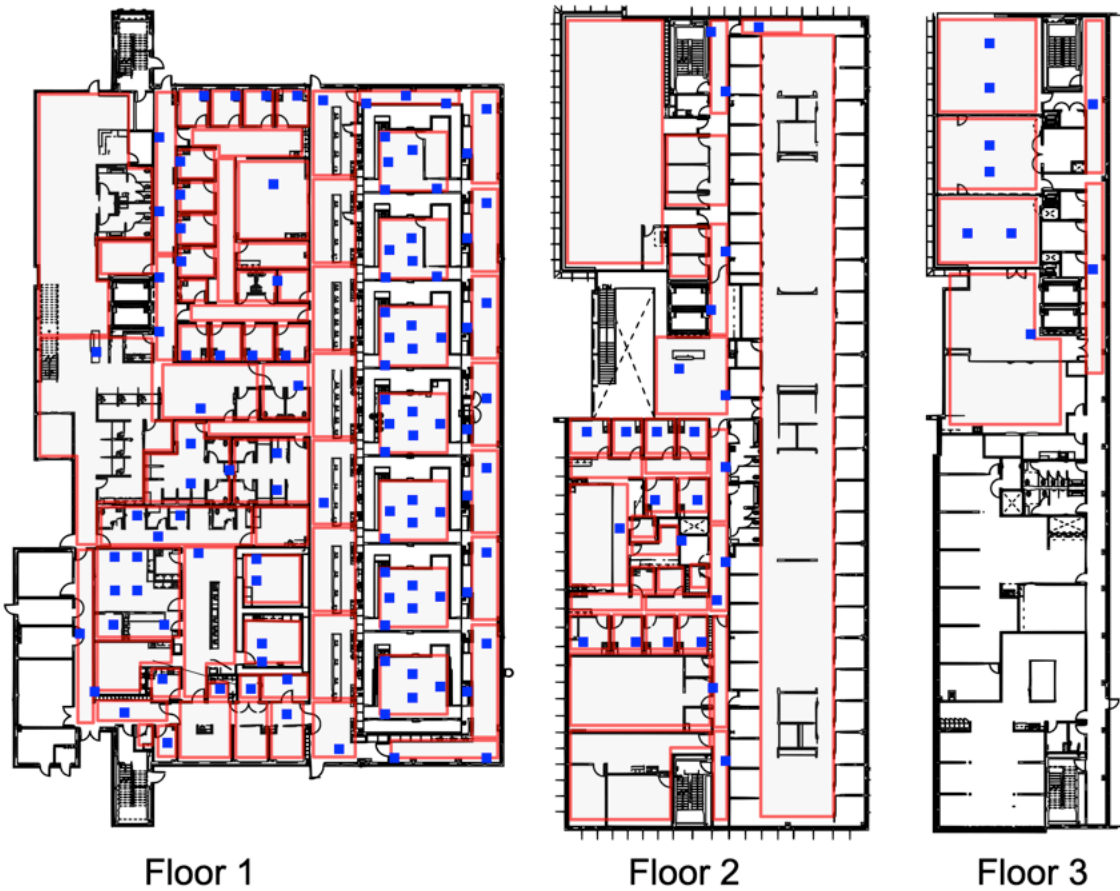


Fig. 2. Floor plan with 115 zones (red-board boxes) and 142 BLE scanners (blue squares).

Because of the strong interference and missing data during intervals in which BLE scanners switch among the three BLE channels (2402, 2426, and 2480 MHz), the BLE signals received fluctuate substantially and are incomplete. Thus, we take the average of the signal strength every 5 seconds to reduce the effects of fluctuation and incompleteness. The beacon tags are set to broadcast messages with an interval of 0.1 second. Thus, we take the average of about every 50 timesteps. Averaging over longer periods further reduces fluctuation but increases location delay.

We use different broadcast intervals for different types of tracked objects, based on how often they move and the clinical requirement for responsiveness, to balance battery life and clinical needs. For example, most facilities rarely move, and the requirement for timing in clinical applications is low. Therefore, we set the broadcast interval to be 1 second and take the average every 50 seconds to calculate location. Patients move more frequently, and the requirement for timing in clinical applications, such as automatic exam room registration and treatment room safety check, is higher. Therefore, we set the broadcast interval for patients to be 0.1 second and take the average every 5 seconds to calculate location. Staff also move more frequently, but the requirement for timing is lower. In addition, longer battery life is more important for staff than for

patients, because the former stay in the hospital much longer than the latter (several years vs. 1-2 months). Therefore, we set the broadcast interval to be 1 second for staff and take the average every 50 seconds to calculate their location, as with facilities.

2.3 Machine learning algorithms

As mentioned above, we use a trained deep learning algorithm to calculate locations. This is a classification problem whose input is the 50-timestep-averaged 142-dimensional vectors, and whose output is the corresponding zone. The vector elements are the signal strength (Received Signal Strength Indicator [RSSI], ranging from approximately -100 to -30) measured from all BLE sensors for each beacon tag. In addition to the last 50-timestep signal, historical locations are useful for constraining the current location because objects can only move at a reasonable velocity. For example, one cannot suddenly move from one corner of the building to another corner 50 m away within 5 seconds. Additionally, some zones are connected to each other with no wall in between, such as two adjacent consoles, or connected with a door in between, such as an exam room and a corridor, whereas other zones are unconnected, such as two adjacent rooms separated by a wall or two zones far from each other. It generally takes less time for an object to move to a connected zone than to an unconnected zone. Considering these factors, a Long Short-Term Memory (LSTM) [24] Recurrent Neural Network (RNN) followed by a multi-class classifier is a natural choice. RNN is a type of neural network that include nodes from previous steps when processing current input data; thus, it can process temporal sequences. For the location problem, current location depends partially on previous locations because of the finite speed limit of objects, and this forms trajectories or temporal sequences. Thus, we use an RNN, which automatically considers historical location and zone connection information, to train on trajectories. LSTM is a type of RNN that partially solves the exploding and vanishing gradient problems encountered by conventional RNNs. It has been widely used in the fields of natural language processing [25] [26] and video processing [27] [28], which primarily deal with unsegmented sequences. Figure 3 illustrates the network architecture, which includes an embedded LSTM and a multi-class classifier (here, a multilayer perceptron classifier) for our RTLS's location computation. Each input vector is a 50-timestep-averaged 142-dimensional vector of the BLE RSSI of a beacon tag. The output is the zone of the tag within the last 50 timesteps. Note that the output interval is 10 timesteps, because we take a 50-timestep sliding-window average every 10 timesteps. We use the sliding window scheme to reduce noise while maintaining a reasonably high update rate. The classifier is composed of 2 fully-connected dense layers, each with a "ReLU" activation and, eventually, a "softmax" layer to calculate the probability of each zone. The zone with the highest probability is the final result.

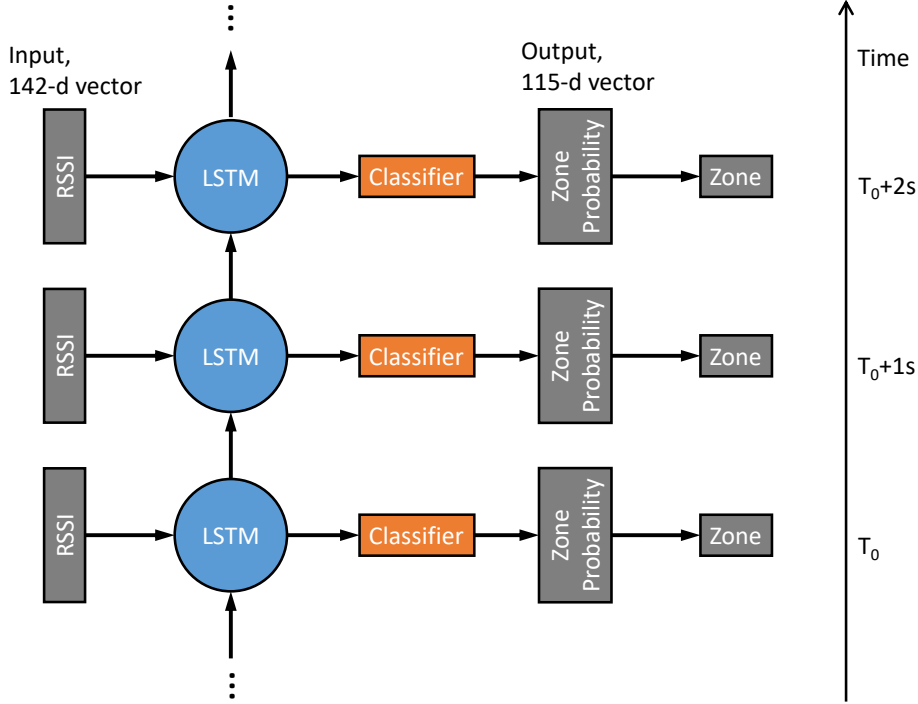


Fig. 3. Illustration of the LSTM-classifier Neural Network for location computation.

2.4 Data collection and experiments

To collect training and testing data, we carried beacon tags around each zone and collected the raw signal strength data and corresponding zones. The tags were carried in front of the chest using a lanyard, in the shirt pocket, or in the pant pocket to mimic different scenarios for real patients. We walked randomly but tried to go through all positions and corners in each zone to reduce gaps between classes. Some areas are occupied by large facilities such as tables, desks, and exam chairs; in such cases, we took the tag out and carried it in our hands to go over these areas. In one of our two experiments, we carried 6 tags in different body positions to collect the training set, and we carried 1 additional tag to independently collect a testing set. For each zone, we collected data for 2 minutes with approximately 1200 timesteps, considering the BLE broadcast interval of 0.1 second. To test the robustness and responsiveness in real-world cases, we collected 10 trajectories in the second experiment, during which we carried the tag across zones. Each trajectory was about 20 minutes, and it encountered 20-30 cross-zone events. The ground truth locations were collected using real-time location.

2.5 Data augmentation

To predict trajectories involving zone crossings, we augmented data to generate training sequences for LSTM. We used a memory of 6 steps for LSTM, which is equivalent to 100-timestep memory, considering the 10-timestep update interval and the 50-timestep sliding window. Within 100 timesteps, it is rare for a person to walk very far. Thus, our training sequences are either within

a single zone or between two connected zones. Sequences within a single zone were taken from the sequences collected in the training set. For sequences between two connected zones, we randomly selected n instances from one zone and $10-n$ instances from the other zone and concatenated them. We note that these augmented cross-zone sequences are artificial, but they provide an opportunity to see whether LSTM can improve location accuracy in real-world scenarios, where zone-crossing events are common.

2.6 Posterior constraint

LSTM with augmented training data takes artificial cross-zone sequences as input, but it may not effectively predict real-world cross-zone trajectories. Thus, to better account for the historical location information and zone-connection information, the machine learning model's output (a vector of zone probabilities) is postprocessed to use the previous zone and zone connection information to constrain the current zone (Eq. 1):

$$P(Z_t^n | Z_{t-\Delta t}^m) = \frac{P(Z_t^n) P(Z_{t-\Delta t}^m | Z_t^n)}{P(Z_{t-\Delta t}^m)}, \quad (1)$$

where $P(Z_t^n)$ is the probability of the n^{th} ($n=1,2,\dots,115$) zone calculated from the model at time t , and $P(Z_{t-\Delta t}^m)$ is the probability of the m^{th} ($m=1,2,\dots,115$) zone in the previous time step $t - \Delta t$. For simplicity, we assume the previous zone is known, so that

$$P(Z_{t-\Delta t}^m) = 1. \quad (2)$$

The conditional probability $P(Z_{t-\Delta t}^m | Z_t^n)$ is assumed as

$$P(Z_{t-\Delta t}^m | Z_t^n) = k^{-d_{mn}/\Delta t}, \quad (3)$$

where d_{mn} is the distance between the n^{th} zone (candidate current zone) and the m^{th} zone (previous zone) (defined as the minimum number of crosses between two zones, e.g., between two connected zones is 1, and between the same zone is 0 when $m=n$), and Δt is the time difference between the current timestep and the previous timestep in seconds ($\Delta t = 1$ for non-disturbed tracking of patients). $P(Z_t^n)$ is directly calculated from the machine learning classifier. Eventually, the maximum of $P(Z_t^n | Z_{t-\Delta t}^m)$ is taken to predict the zone at time t . Equation (3) indicates that it is less probable that a patient will show up in a zone far away from the previous zone, but this spatial probability constraining effect diminishes over time. For example, the longer the time since the last known location, the more likely it is that the patient will show up in a zone far from the previous known zone. Note that errors in computing the previous zone can affect the current zone computation, because, in real-time prediction, the ground truth is unknown for both the current

and the previous steps. Thus, parameter k should be carefully optimized so that the constraint is effective and also that the effect of errors from the previous location calculation can be reduced when calculating the current zone. Note also that the equation assumes that the probability of all zone-crossings is equal. Since we don't have data for real-time patients, the number k is given an empirical value, which indicates the probability of a patient staying compared to moving. Additionally, the minimum number of crossings between two zones is not exact but an approximation of their distance. However, we use a posterior constraint scheme that relies heavily on approximation along with the classifier to predict the trajectory, and we reasonably expect to see an improvement in robustness. Figure 4 illustrates the LSTM+constraint scheme, which accounts for information from previous steps better than LSTM. We will compare the performance of these methods in terms of their accuracy, robustness, and responsiveness.

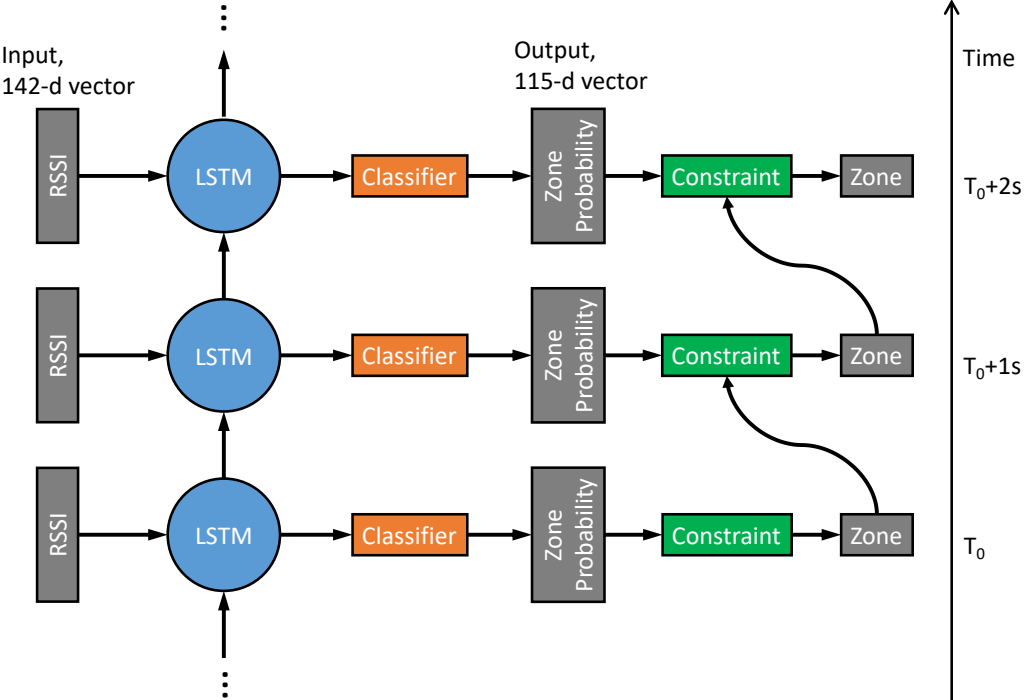


Fig. 4. Illustration of an MLP-constraint Neural Network structure for location computation.

2.7 Baseline methods

As a baseline to compare with LSTM, we implemented Support Vector Machine (SVM) and Multilayer Perceptron (MLP) schemes as well. The MLP is the same classifier used in the LSTM network presented above. We also implemented the previously developed CNN+ANN model [12] for comparison. Note that we are dealing with multi-floor localization instead of a single floor, as in Iqbal et al.'s paper [12]; we modified the CNN method to use 3D convolutional layers.

3. Results

We first evaluated schemes in terms of their accuracy for separate zones, neglecting cross-zone events. Among the 6 tags, we selected 5 as the training set and the other 1 as the validating set. Thus, for each scheme we performed 6 training-validation experiments and computed the average and standard deviation of the accuracy. Finally, we used an additional 1 tag as the testing set to test the generality of the schemes. For LSTM, the memory length was set as 6 timesteps. Table 1 shows the cross-validation and test accuracy of each scheme. It is clear that LSTM outperforms SVM and MLP when no cross-zone events are encountered. Meanwhile, MLP presents higher accuracy than SVM. As a baseline for comparison, we also implemented the CNN+ANN scheme developed by Iqbal et al. [12]. The history length is 5 seconds, the same as MLP. The CNN+ANN scheme achieved similar accuracy to MLP, outperformed SVM and underperformed LSTM. Note that the CNN+ANN scheme in our experiment is less accurate than in the initial report [12], because that paper focused on a much smaller area (first floor top center) where the sensors are relatively dense; the zones in that paper are also larger than in our experiments.

Table 1 Cross-validation accuracy and test accuracy of four schemes.

Methods	Cross-validation accuracy (%)	Test accuracy (%)
SVM	92.9 ± 2.6	94.1
CNN+ANN	94.3 ± 2.5	95.7
MLP	94.1 ± 2.2	95.2
LSTM	97.2 ± 1.5	97.1

Figure 5 shows the accuracy distribution of LSTM in the building. In clinical exam areas (i.e., top center of the first floor and middle left of the second floor), where the sensors are relatively dense, the accuracy is higher than in areas where the sensors are relatively sparse. On the other hand, larger zones (e.g., third floor) are more easily classified than smaller zones. Though not mathematically quantified, we can briefly conclude from the figure that the number of sensors should be close to or more than the total number of zones to achieve good accuracy. LSTM achieves an overall accuracy of about 97%. However, for most clinical areas, the accuracy is 100% or close to it. There are a few zones where the accuracy is low, but most of them are considered unimportant (e.g., corridors) for clinical applications. These low-accuracy areas also have a low density of sensors. We can install more sensors in these areas to increase accuracy if necessary.

zone sequences. To compensate for this, we augmented the training data to include cross-zone sequences. For each connected-zone pair, we randomly selected data from each zone and concatenated them to form a sequence. Such a sequence mimics a trajectory from one zone to a connected zone. Because our memory length is 6, relatively short (10 seconds in total), we limited all sequences to at most two zones. In doing so, we were able to mimic cross-zone sequences.

Figure 6 illustrates using different methods to predict the location of a testing trajectory that involves 15 zones in the exam room area in the first floor of EROC and 24 cross-zone events. The plot shows the zone variation with time steps. We show the results of LSTM and LSTM with augmentation and constraint. Among the methods, LSTM+augmentation had the most incorrect zone changes (42), while the MLP+constraint with $k=40$ had the fewest incorrect zone changes (0). The latter method is more robust than the former. We also noted that most zone changes happened during or close to zone crossings. This is reasonable, partly because classification tends to be ambiguous at class boundaries (e.g., when standing at the door) so the training data may not distinguish effectively between two connected zones, and partly because the 5-second averaging window lies in both zones, and the training data do not cover such cross-zone window. However, averaging across fewer seconds increases the noise (not shown); under these conditions, the method still cannot distinguish zones well, but its robustness is worse. Therefore, we stayed with the 5-second average to maintain the balance between robustness and ambiguity.

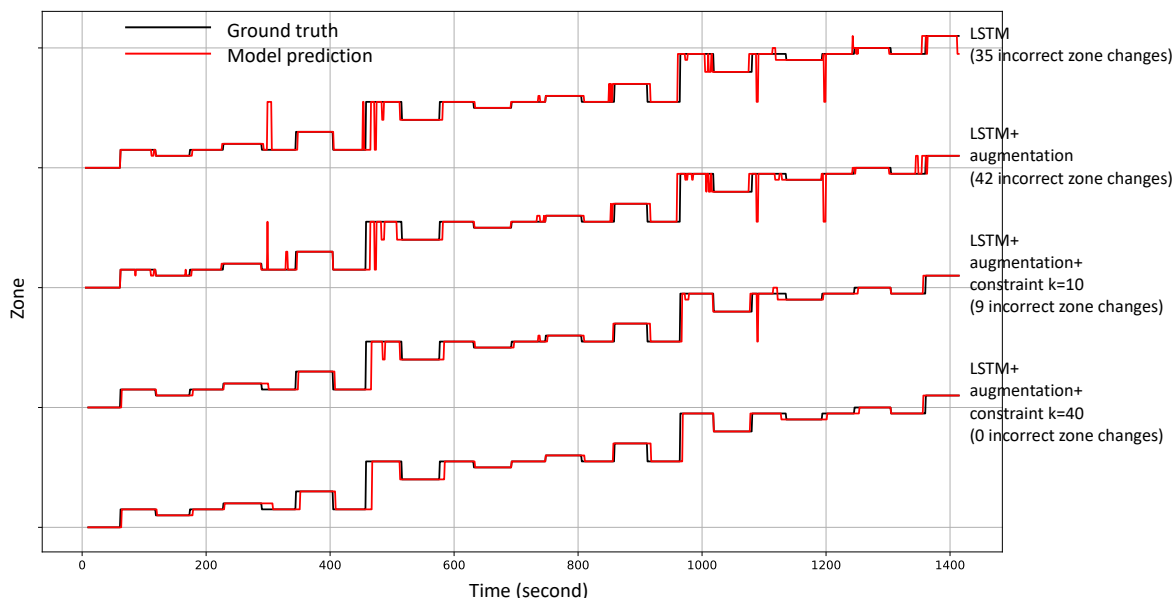


Fig. 6. Performance of LSTM, LSTM+augmentation and LSTM+augmentation+constraint with $k=10$ and $k=40$ for predicting an example trajectory. Y axis is zone, and X axis is time (seconds).

LSTM+augmentation is less robust than LSTM presumably because the augmented training data involves cross-zone sequences, while the original training data for LSTM involves

only in-zone sequences. That said, LSTM+augmentation tends more to predict leaving previous zones than LSTM. Thus, LSTM+augmentation is less robust but more responsive than LSTM.

Figure 6 also shows that increasing k in LSTM+augmentation+constraint leads to more robust localization. This is because, with a larger k , the algorithm is more likely to predict staying in the previous zone than leaving, according to Equations (1-3). Thus, when ambiguous, the model tends to predict staying in the previous zone until it is sure that the object has left the zone.

To quantify robustness and responsiveness, we define degree of robustness as

$$RO = 1 - \frac{N_p^{change} - N_g^{change}}{N_p^{change} + N_g^{change}}, \quad (4)$$

where N_g^{change} and N_p^{change} are the number of zone changes in the ground truth and predicted trajectories, respectively. According to this definition, more incorrect zone changes lead to a lower degree of robustness. We define the lagging Δt using a moving minimization:

$$\min_{\Delta t} \sum_t \text{sgn}(|zone_p(t - \Delta t) - zone_g(t)|), \quad (5)$$

where $zone_p(t)$ and $zone_g(t)$ are the predicted and ground truth zones as a function of time, respectively. Using these definitions, we calculated the degree of robustness and lagging. Table 2 shows the degree of robustness and lagging for the four schemes. LSTM+augmentation+constraint, with $k=40$, has the best robustness and a moderate responsiveness, while LSTM+augmentation has the best responsiveness but the worst robustness. With the augmentation scheme added, increasing k (LSTM+augmentation is equivalent to LSTM+augmentation+constraint with $k=0$) leads to better robustness and worse responsiveness. This is consistent with the previous discussion. Without augmentation, LSTM has much greater lagging but not very good robustness: for example, LSTM+augmentation+constraint with $k=40$ is both more robust and more responsive than LSTM and other methods.

Because lagging accounts for part of the error in predicting trajectories, we defined a delay-corrected accuracy to exclude the effect of delay, so we could measure the other part of the error when delay is not the major concern. To do this, considering that every zone change has a different delay, we followed Equation (5) to calculate the delay in predicting zone change, but we confined t to a range of $[-10, 10]$ around every ground truth zone change, meaning we considered the delay to be limited to within 10 seconds; delay over 10 seconds will still be included in the delay-corrected error. Then, we compared the predicting and the delay-adjusted ground truth trajectories to obtain the delay-corrected accuracy. The results are shown in Table 2. The LSTM+augmentation+constraint with $k=40$ achieved 100% accuracy after correcting for the delay. This means that the method is very robust and accurate, but a bit lagging. Although most of our trajectories were collected in clinical areas where the accuracy is high, the delay-corrected

accuracy for the other methods is not as high as the in-zone accuracy shown in Table 1. This is presumably because, in trajectories, the tags are more often in between two zones, which yields more ambiguity.

Table 2 Degree of robustness and lagging of various methods.

Methods	Degree of Robustness	Lagging (seconds)	Delay-corrected accuracy (%)
SVM	0.3	2.4	93.8
CNN+ANN	0.4	2.6	94.6
MLP	0.4	2.4	94.4
LSTM	0.7	4.8	95.7
LSTM+augmentation	0.6	2.4	96.2
LSTM+augmentation+constraint k=10	0.8	3.0	98.1
LSTM+augmentation+constraint k=40	1.0	3.3	100.0

4. Discussion and Conclusions

We evaluated a few machine learning schemes for a BLE-based indoor Real-time Location System built in the Department of Radiation Oncology at the University of Texas Southwestern Medical Center. Because of the noisy nature of BLE signals, using simple classifiers is insufficient for robust localization that can be used in downstream clinical applications. Even a history-based LSTM scheme with data augmentation to predict trajectories still predicts jumping results. To overcome this robustness problem, we developed a posterior constraint algorithm based on historical location and zone connection information. LSTM with this posterior constraint algorithm substantially increased the classifier’s robustness with only a minimal sacrifice of responsiveness. The posterior constraint algorithm controls how likely the object is to leave rather than stay in the previous zone. In real applications, the parameter k should be adjusted to meet the preference of different applications. Some applications (e.g., auto patient check-in for exam rooms) prefer higher robustness to responsiveness, while other applications may prefer higher responsiveness to robustness. For example, to inspect who may have been infected during a certain time period in a certain room according to the historical location records, it is better to include all people who have any chance of being infected. In this case, a higher responsiveness is preferred.

LSTM is a widely used artificial network for predicting unsegmented sequences, and it is good for predicting trajectories. We generated training trajectories using single-zone collections and augmented them to obtain cross-zone trajectories between connected zones. In our experiments, LSTM outperformed all traditional classification methods. This is because LSTM already takes into account historical information. LSTM+augmentation also considers the zone connection information. Thus, a well-trained end-to-end LSTM+augmentation scheme has great potential to improve robustness. However, in our experiments, LSTM+augmentation didn’t

succeed in improving robustness. This could be due to the artificial training trajectories, which didn't include data of zone-crossing at class boundaries. This is the main cause of most ambiguities. Using a collection of real trajectories as training sequences may improve the robustness of LSTM, but the data collection is tedious. Thus, considering that the LSTM+augmentation has not fully explored the zone connection information, we simply applied the constraint technique to it to strengthen the effect of historical location and zone connection information. We found that the LSTM+augmentation+constraint achieves robustness and responsiveness that are both better than LSTM and accuracy that is better than all other tested methods when correcting for the delaying error.

We also tried to improve LSTM+augmentation by adjusting memory length. However, longer memory didn't improve robustness or responsiveness. This could still be due to the artificial training sequences, which may not represent real trajectories well.

We found that zones where BLE sensors are sparse have lower accuracy than those where sensors are dense, and larger zones tend to have higher accuracy than smaller zones. Thus, during deployment, one may consider combining unimportant offices into larger zones and increasing sensor density to increase accuracy. From our experience, the total number of sensors should be similar to or greater than the total number of zones to achieve good accuracy. The density of sensors should also be similar to the density of zones. An easy implementation method would be to install one sensor in each zone.

The parameter k in the constraint scheme controls the probability that the tracked object will stay in its previous location. Increasing k results in more robust tracking, while decreasing k results in more responsive tracking. Most applications prefer robust results. Thus, we set k to achieve maximum robustness. However, k should not be too large, or else errors from previous location computations may transfer to the next location computation without being eliminated effectively, which would lead to weak responsiveness. From our experience, k should be between 20-200 for a good balance between robustness and responsiveness.

Decreasing the averaging window may increase responsiveness. However, doing so also decreases accuracy and robustness significantly. The constraint scheme requires a small location error because it assumes that the previous location error is small. Smaller windows lead to larger location errors, which transfer to the next step and make the constraint scheme less effective. Increasing the averaging window may increase robustness, but it may also reduce responsiveness, and the k parameter should also be re-optimized because the error changes. Further systematic analysis is necessary to optimize the window and the k parameter to achieve the best balance between robustness and responsiveness.

The walls and doors of treatment rooms are thick enough to completely block BLE signals. Thus, opening and closing treatment room doors leads to big differences in the received signal strength when the sensor and beacon tag are on opposite sides of the door. We noticed in our experiments that the model trained using data collected when treatment room doors were closed is less accurate for testing data collected when the doors are open, especially for zones close to the

treatment rooms. This is presumably because the testing data included sensors from both sides of the doors, but these were not covered by the training data. To overcome this shortcoming, we collected the training data again leaving all treatment room doors open. In this case, the training data covered the testing data much better. We noticed that “normal” doors (on non-treatment rooms) have much less of an effect on the signals and merge into many other sources of noises. Thus, we don’t pay special attention to the normal doors.

We have made many assumptions and approximations in our schemes. The distance between two zones defined in this paper is not precise but briefly reflects the real distance. The probabilities of crossing between two connected zones are all assumed to be equal. The previous zone is assumed to be known in the constraint scheme. The effectiveness of the schemes has to be tested further with more data.

Infrastructure and environments change over time, and this will affect the function mapping the signal footprint to location. For example, the EROC building has built and demolished a few inner walls since we collected the training data. This affects the real-time testing accuracy, especially for zones close to the changed walls. Thus, we suggest periodically re-collecting training data and re-training the model.

In summary, we have developed an RTLS to accurately track patient, staff, and equipment in clinic environments, and, by employing deep learning technique we have achieved high accuracy in predicting trajectories of moving objects. Clinical applications will be developed based on the present RTLS.

Acknowledgement

The authors acknowledge Erlei Zhang for useful discussion of algorithms. The authors thank Jonathan Feinberg for editing the manuscript.

References

- [1] J. Borenstein and Y. Koren, "Real-time obstacle avoidance for fast mobile robots," *IEEE Transactions on systems, Man, and Cybernetics*, vol. 19, no. 5, pp. 1179-1187, 1989.
- [2] D. Oosterlinck, D. Benoit, P. Baecke and N. Van de Weghe, "Bluetooth tracking of humans in an indoor environment: An application to shopping mall visits," *Applied geography*, vol. 78, pp. 55-65, 2017.
- [3] T. Jones and C. Schlegel, "Can real time location system technology (RTLS) provide useful estimates of time use by nursing personnel?," *Research in nursing & health*, vol. 37, no. 1, pp. 75-84, 2014.
- [4] M. Boulos and G. Berry, "Real-time locating systems (RTLS) in healthcare: a condensed primer," *International journal of health geographics*, vol. 11, no. 1, p. 25, 2012.

- [5] J. Van Hoof, J. Verboor, C. Oude Weernink, A. Sponselee, J. Sturm, J. Kazak, G. Govers and Y. van Zaalén, "Real-time location systems for asset management in nursing homes: An explorative study of ethical aspects," *Information*, vol. 9, no. 4, p. 80, 2018.
- [6] M. Boulos and G. Berry, "Real-time locating systems (RTLS) in healthcare: a condensed primer," *International journal of health geographics*, vol. 11, no. 1, p. 25, 2012.
- [7] B. Wang, M. Toobaie, R. Danskin, T. Ngarmnil, L. Pham and H. Pham, "Evaluation of RFID and Wi-Fi technologies for RTLS applications in Healthcare Centers," *2013 Proceedings of PICMET'13: Technology Management in the IT-Driven Services (PICMET)*, pp. 2690-2703, 2013.
- [8] Y. Bendavid, "RFID-enabled Real-Time Location System (RTLS) to improve hospital's operations management: An up-to-date typology," *International Journal of RF Technologies*, vol. 5, no. 3-4, pp. 137-158, 2013.
- [9] S. Porto, C. Arcidiacono, A. Giummarra, U. Anguzza and G. Cascone, "Localisation and identification performances of a real-time location system based on ultra wide band technology for monitoring and tracking dairy cow behaviour in a semi-open free-stall barn," *Computers and Electronics in Agriculture*, vol. 108, pp. 221-229, 2014.
- [10] D. Dardari, N. Decarli, A. Guerra and F. Guidi, "The future of ultra-wideband localization in RFID," *IEEE International Conference on RFID (RFID)*, pp. 1-7, 2016.
- [11] A. Alarifi, A. Al-Salman, M. Alsaleh, A. Alnafessah, S. Al-Hadhrami, M. Al-Ammar and H. Al-Khalifa, "Ultra wideband indoor positioning technologies: Analysis and recent advances," *Sensors*, vol. 16, no. 5, p. 707, 2016.
- [12] Z. Iqbal, D. Luo, P. Henry, S. Kazemifar, T. Rozario, Y. Yan, K. Westover, W. Lu, D. Nguyen, T. Long and J. Wang, "Accurate real time localization tracking in a clinical environment using Bluetooth Low Energy and deep learning," *PloS one*, vol. 13, no. 10, p. e0205392, 2018.
- [13] G. Mendoza-Silva, M. Matey-Sanz, J. Torres-Sospedra and J. Huerta, "BLE RSS Measurements Dataset for Research on Accurate Indoor Positioning," *Data*, vol. 4, no. 1, p. 12, 2019.
- [14] M. Bowen, J. Craighead, C. Wingrave and W. Kearns, "Real-time locating systems (RTLS) to improve fall detection," *Gerontechnology*, vol. 9, no. 4, p. 464, 2010.
- [15] J. Hallberg, M. Nilsson and K. Synnes, "Positioning with bluetooth," in *In International Conference on Telecommunications: Special Session on IoT Emerging Technologies: Design and Security (ITEMS'16) 16/05/2016-18/05/2016*, 2003.
- [16] M. Collotta, G. Pau, T. Talty and O. Tonguz, "Bluetooth 5: A concrete step forward toward the IoT," *IEEE Communications Magazine*, vol. 56, no. 7, pp. 125-131, 2018.

- [17] F. Topak, M. Pekerikli and A. Tanyer, "Technological Viability Assessment of Bluetooth Low Energy Technology for Indoor Localization," *Journal of Computing in Civil Engineering*, vol. 32, no. 5, p. 04018034, 2018.
- [18] B. Clark, E. Winkler, C. Brakenridge, S. Trost and G. Healy, "Using Bluetooth proximity sensing to determine where office workers spend time at work," *PloS one*, vol. 13, no. 3, p. e0193971, 2018.
- [19] R. Faragher and R. Harle, "An analysis of the accuracy of bluetooth low energy for indoor positioning applications," *Proceedings of the 27th International Technical Meeting of the Satellite Division of the Institute of Navigation (ION GNSS+2014)*, vol. 812, 2014.
- [20] N. Agarwal, J. Basch, P. Beckmann, P. Bharti, S. Bloebaum, S. Casadei, A. Chou, P. Enge, W. Fong, N. Hathi and W. Mann, "Algorithms for GPS operation indoors and downtown," *GPS solutions*, vol. 6, no. 3, pp. 149-160, 2002.
- [21] Y. Wang, X. Yang, Y. Zhao, Y. Liu and L. Cuthbert, "Bluetooth positioning using RSSI and triangulation methods," in *2013 IEEE 10th Consumer Communications and Networking Conference (CCNC)*, 2013.
- [22] S. Feldmann, K. Kyamakya, A. Zapater and Z. Lue, "An indoor bluetooth-based positioning system: Concept, implementation and experimental evaluation," in *International Conference on Wireless Networks*, 2003.
- [23] Y. LeCun, Y. Bengio and G. Hinton, "Deep learning," *Nature*, vol. 521, no. 7553, p. 436, 2015.
- [24] S. Hochreiter and J. Schmidhuber, "Long short-term memory," *Neural computation*, vol. 9, no. 8, pp. 1735-1780, 1997.
- [25] K. Yao, B. Peng, Y. Zhang, D. Yu, G. Zweig and Y. Shi, "December. Spoken language understanding using long short-term memory neural networks," in *2014 IEEE Spoken Language Technology Workshop (SLT)*, 2014.
- [26] J. Gonzalez-Dominguez, Lopez-Moreno, I., H. Sak, J. Gonzalez-Rodriguez and P. Moreno, " Automatic language identification using long short-term memory recurrent neural networks," in *Fifteenth Annual Conference of the International Speech Communication Association*, 2014.
- [27] K. Zhang, W. Chao, F. Sha and K. Grauman, "Video summarization with long short-term memory," in *European conference on computer vision*, 2016.
- [28] J. Yue-Hei Ng, M. Hausknecht, S. Vijayanarasimhan, O. Vinyals, R. Monga and G. Toderici, "Beyond short snippets: Deep networks for video classification," in *Proceedings of the IEEE conference on computer vision and pattern recognition*, 2015.

- [29] R. Arroyo, J. Yebes, L. Bergasa, I. Daza and J. Almazán, "Expert video-surveillance system for real-time detection of suspicious behaviors in shopping malls," *Expert systems with Applications*, vol. 42, no. 21, pp. 7991-8005, 2015.
- [30] N. Bulusu, J. Heidemann and D. Estrin, "GPS-less low-cost outdoor localization for very small devices," *IEEE personal communications*, vol. 7, no. 5, pp. 28-34, 2000.